A&A 532, A137 (2011)
DOI: 10.1051/0004-6361/201117358

Astronomy & Astrophysics

Transport and diffusion of particles due to transverse drift waves

J. Vranjes

Belgian Institute for Space Aeronomy, Ringlaan 3, 1180 Brussels, Belgium
e-mail: jvranjes@yahoo.com

Received 27 May 2011 / Accepted 8 July 2011

ABSTRACT

Transport and diffusion of plasma particles perpendicular and parallel to the magnetic field is discussed in the framework of the transverse drift wave theory. The starting model includes the density and magnetic field gradients perpendicular to the magnetic field vector. In such an inhomogeneous environment the transverse drift wave naturally develops. The transverse drift wave is a low frequency mode, with the frequency far below the ion gyro-frequency, it is driven by these gradients and it propagates perpendicular to them. The mode is also purely perpendicular to the magnetic field and it is electromagnetically transverse, which implies that when its wave vector is perpendicular to the magnetic field vector, the perturbed electric field is along the equilibrium magnetic field, while in the same time the perturbed magnetic field is in the direction of the background gradients. In application to the solar wind, it is shown that very small wave electric field amplitude, of the order of 10^{-7} V/m, within one wave period can produce the drift of protons in both directions, perpendicular to the ecliptic plane and also along the background magnetic field, to distances measured in millions of kilometers. The electric field along the magnetic field vector implies particle acceleration in the same direction. When a critical threshold velocity of the particle is achieved, the particle motion becomes stochastic. This is a completely new nonlinear stochastic mechanism which follows from the very specific geometry of the transverse drift mode. Particle drift perpendicular to the magnetic field vector means a diffusion of particles, with the effective diffusion coefficient for ions that is at least 11 orders of magnitude larger than the classic diffusion coefficient. The features of this diffusion are: within certain time interval, initially faster particles will diffuse to larger distances, and the same holds for protons in comparison to heavier ions. For electrons the effective diffusion coefficient can easily match the one obtained from observations, i.e., to become of the order of 10^{17} m^2/s. It is also expected that the wave-induced stochastic motion will considerably increase the effective collision frequency in such an environment which is, with respect to its mean parameters, practically collision-lees. Hence, the solar wind regions affected by such a stochastic acceleration may show various unexpected features that are typical for collisional plasmas.

Key words. solar wind – waves – Sun: heliosphere

1. Introduction

The electromagnetic transverse drift mode has been predicted long ago (Krall & Rosenbluth 1963; Krall 1972), yet it was investigated in just a few previous works (Krall & Tidman 1969; Wu et al. 1986). This is a mode driven by the energy stored in the inhomogeneous background plasma with the gradients of the density and the magnetic field perpendicular to the ambient magnetic field vector. In the present work a possible application of the transverse drift mode to the solar wind plasma is presented. The solar wind is in fact an inhomogeneous environment with accidental temporal density inhomogeneities in the direction perpendicular to the magnetic field vector that are dictated by various phenomena in the source, i.e., in the Sun (Bavassano et al. 1978; Tsiklauri et al. 2002). Particle transport in the presence of density gradients perpendicular to both the ecliptic plane and to the magnetic field vector has been discussed in the past (Zhang et al. 2003b). The presence of such a plasma inhomogeneity implies the presence of drift waves, that are known to be driven by the background plasma gradients (i.e., gradients of the density, magnetic field and temperature). The drift wave is frequently called the universally growing mode because it grows in practically any environment, due to kinetic and fluid instabilities, in collision-less and collisional plasmas.

The geometry of the model used here, in the local Cartesian reference frame carried by the solar wind assumes the magnetic field that is either in the ecliptic plane or parallel to it $\boldsymbol{B}_0 = B_0\boldsymbol{e}_z$ following the usual spiral configuration, the wave number vector may be in the same plane or in any other, but it is strictly perpendicular to the magnetic field $\boldsymbol{k} = k\boldsymbol{e}_y$. The gradients of the background magnetic field and the density are perpendicular to the magnetic field, e.g., they are in the ecliptic plane or in any other generally x-direction. All essential properties of the transverse drift mode are described by

$$\boldsymbol{k}\cdot\boldsymbol{B}_0 = 0, \quad \boldsymbol{E}_1 \parallel \boldsymbol{B}_0, \quad \boldsymbol{B}_1 \perp \boldsymbol{B}_0, \quad \boldsymbol{E}_1 \perp \boldsymbol{B}_1. \tag{1}$$

Here, $\boldsymbol{E}_1, \boldsymbol{B}_1$ are the perturbed components of the electromagnetic field. Hence, the perturbed electric field is in the direction of the background magnetic field vector, while the magnetic field perturbation vector is in the x-direction, parallel to the background gradients, and from the Faraday law it is given by $\boldsymbol{B}_1 = (kE_{z1}/\omega)\boldsymbol{e}_x$. The mode propagates perpendicular to both the magnetic and electric field vectors, and to the gradients of the background plasma parameters.

According to plasma parameters in the solar wind, this is a very collision-less environment with the mean free path of particles (according to parameters near the Earth's orbit) that is larger than one astronomical unit. Hence, particles coming from

the Sun, in average, suffer no collisions before coming close to the Earth. In the absence of any additional forces, their trajectories should therefore closely follow the direction of the magnetic field vector, and no diffusion in the perpendicular direction can be expected. These facts introduce also some constraints regarding the theoretical models used for the description of phenomena in the solar wind, like for example the applicability of fluid theory (the issue that is so frequently ignored in the literature) that can be used only for processes that involve scales far exceeding the particle mean free path. Yet, observations in the past have shown large fluxes of solar energetic particles (SEPs) at high latitudes (Wibberenz & Cane 2006; Lario et al. 2003; Maclennan et al. 2003), and perpendicular to the magnetic field in general (Dwyer et al. 1997; Zhang et al. 2003a). The usual cross field diffusion appears to be too slow to explain such events, and the same holds for the random walk of the magnetic field lines (Kóta & Jokipii 1995), and for the shock driven transport. Therefore such fluxes represent a challenge for the theory. Delay of arrival of such particles to high latitudes, as compared to their motion along the magnetic field vector, still seems to suggest that their transport in the direction perpendicular to the ecliptic plane should be due to some diffusion process (Zhang et al. 2003b) that definitely can not be described by classic diffusion theory.

Observations reported earlier (Dwyer et al. 1997) show in fact that the ratio of the perpendicular and parallel diffusion coefficients exceed 0.1, reaching as high values as 1.5. These ratios persisted for time periods measured in hours, and it was suggested that the role of perpendicular transport in the heliosphere should be reexamined. In that particular case, the authors attributed these observations to the high level of Alfvén fluctuations that were also regularly observed. Similar values for the ratio of the diffusion coefficients (i.e., around 0.25) were also reported elsewhere (Zhang et al. 2003a).

2. Basic properties of the transverse drift wave

For relatively large wave-lengths, $k\rho_i < 1$, $\rho_i = v_{Ti}/\Omega_i$, $v_{Ti}^2 = \kappa T_i/m_i$, $\Omega_i = q_iB_0/m_i$, of perturbations that are in the form $\sim f(x)\exp(-\mathrm{i}\omega t + iky)$, and using the usual local approximation $|\mathrm{d}f(x)/\mathrm{d}x| \ll k$, $kL_n, kL_b \gg 1$, where L_n, L_b denote the characteristic inhomogeneity lengths of the density and the magnetic field, $L_n = [(\mathrm{d}n_0/\mathrm{d}x)/n_0]^{-1} \equiv 1/\epsilon_n$, $L_b = [(\mathrm{d}B_0/\mathrm{d}x)/B_0]^{-1} \equiv 1/\epsilon_b$, the frequency and the growth rate of the mode are given by (Krall & Rosenbluth 1963):

$$\omega_r = -\frac{k\kappa T_\mathrm{e}}{en_0B_0}\frac{\mathrm{d}n_0}{\mathrm{d}x}\frac{1}{1+k^2c^2/\omega_\mathrm{pe}^2}, \tag{2}$$

$$\frac{\gamma}{\omega_r} = \pi\frac{m_\mathrm{e}}{m_i}\frac{\epsilon_n}{\epsilon_b}\left(1+\frac{k^2c^2}{\omega_\mathrm{pe}^2}\right)^{-2}\left(1+\frac{k^2c^2}{\omega_\mathrm{pe}^2}+\frac{T_\mathrm{e}}{T_i}\right) \times \exp\left\{-\frac{\epsilon_n}{\epsilon_b}\frac{T_\mathrm{e}}{T_i}\frac{1}{1+k^2c^2/\omega_\mathrm{pe}^2}\right\}. \tag{3}$$

Compared to typically strongly growing oblique drift wave described elsewhere (Vranjes & Poedts 2006, 2009a,b), the transverse mode, although always unstable, is not a fast growing mode. However, in the solar wind environment the growth rate of the transverse drift mode can sometimes become greater than the growth rate of the oblique drift wave. In addition, it can become very strongly growing in the presence of an electron temperature anisotropy, $T_\perp < T_\parallel$, where $\perp$ and $\parallel$ denote, respectively, directions perpendicular to the magnetic field and parallel to it (Wu et al. 1986). The instability can also become stronger with the simultaneous presence of the temperature gradient (Mikhailovskii 1992), especially in the limit of a small plasma-β. The frequency in that case is similar as above, but the growth rate is multiplied by the factor $1 + (2/\beta)[\eta/(1+\eta)]$, $\eta = [\mathrm{d}T/(T\mathrm{d}x)]/[\mathrm{d}n/(n\mathrm{d}x)]$. This factor can be large in plasmas with small plasma-β; although this is not a typical situation in the solar wind, it is possible.

However, because of its specific geometry, having large amplitudes (i.e., a strong growth) of the mode is not so essential. To test the wave behavior and the particle motion in the wave field, unless otherwise stated, the following solar wind plasma parameters typical for the distance of 1 AU from the Sun (Gosling 2007) will be used: $T_i \simeq T_\mathrm{e} = 1.5\times10^5$ K, $n_{i0} = n_{\mathrm{e}0} = n_0 = 5\times10^6$ m^{-3}, $B_0 = 5\times10^{-9}$ T. The ions are singly charged protons and we also postulate $L_n = 10^8$ m. The wave-length is taken $\lambda = 10^6$ m so that the plasma is magnetized and the local approximation reasonably well satisfied. For the given parameters the plasma-β is 1.04, $\rho_i = 74\times10^3$ m, $\Omega_i \simeq 0.5$ Hz, and from Eq. (2) we have $\omega_r = 0.00016$ Hz and therefore the wave period $T_w \simeq 3.8\times10^4$ s which is around 10.7 h. Hence, the drift approximation $\omega_r/\Omega_i \ll 1$ is very well satisfied. Because $L_n/L_B = \beta/2$ (Vranjes 2011), we have $L_b = 1.9\times10^8$ m.

The obtained frequency is rather arbitrary and in principle one can start from any other value. Obviously, the parameters used here can be varied to obtain even longer, and shorter (of about one hour) wave periods. Note however that, because $\omega_r \sim kT_\mathrm{e}/(B_0L_n)$, the obtained frequency will keep the same value for a large span of these parameters. While all four parameters can be varied, this is especially applicable for k and L_n; as long as the ratio k/L_n remains the same, the frequency will remain the same too. So the results presented further in the text, although obtained for one fixed frequency for the purpose of demonstration only, are in the same time valid for a large span of parameters. In some limit though (for larger k), the condition $k\rho_i < 1$ becomes violated, yet this only implies using another similar expression for the wave frequency (Krall & Rosenbluth 1963; Krall 1972), obtained within the appropriate wavelength range and through a different expansion with respect to the parameter $k\rho_i$. In any case, the mode behavior will remain the same or similar.

In view of the assumed geometry, the particle gyration around the magnetic field vector is in the plane perpendicular to the ecliptic, while its starting displacement due to the wave is primarily in the ecliptic plane or parallel to it, and it is along the wave electric field vector, which is parallel to $\boldsymbol{B}_0$. It will be shown that a large particle drift will also develop perpendicular to the ecliptic, i.e.., in the x-direction.

Observe that for the given parameters, the ion collision frequency $\nu_{ii} = 4n_{i0}(\pi/m_i)^{1/2}[e_i^2/(4\pi\varepsilon_0)]^2L_{ii}/[3(\kappa T_i)^{3/2}]$ is about 1.4×10^{-7} Hz, and the ion mean free path is therefore 2.6×10^{11} m, i.e., around 1.7 astronomical units. The classic perpendicular ion diffusion coefficient (Chen 1988) is $D_\perp \approx \kappa T_i\nu_i/(m_i\Omega_i^2) = 736$ m^2/s and the corresponding diffusion velocity in the direction of the given density gradient is $v_D = D_\perp\nabla n/n = 7\times10^{-6}$ m/s only. Hence, the classic collisional diffusion is totally negligible because within the given wave period the mean diffusion distance for a proton is only 0.3 m. One can try with the Bohm diffusion coefficient $D_B = \kappa T_\mathrm{e}/(16eB_0)$, which for the given parameters in the solar wind is considerably larger and it is around 1.6×10^8 m^2/s. It will be shown below that this is still far below the effective diffusion caused by the transverse drift waves.

3. Single particle motion in the wave field

Dynamics of a single particle in the given transverse sinusoidal drift wave field is described by

$$\frac{\mathrm{d}\boldsymbol{v}}{\mathrm{d}t} = \frac{q}{m}\left[\boldsymbol{E}(\boldsymbol{r},t) + \boldsymbol{v}\times\boldsymbol{B}(\boldsymbol{r},t)\right]. \tag{4}$$

For the y, z components in the cartesian geometry this yields

$$y'' + \Omega^2 y - [qkv_z\widehat{E}_{z1}/(m\omega)]\sin(-\omega t + ky) = 0, \tag{5}$$

$$z'' - (1 - ky'/\omega)(q\widehat{E}_{z1}/m)\sin(-\omega t + ky) = 0. \tag{6}$$

Here, the prime denotes the time derivative, and the electric field E_{z1} is sinusoidal with the amplitude $\widehat{E}_{z1}$. Eq. (5) is a combination of the x and y components, and it is obtained after one integration of the corresponding x-component $x'' = \Omega y'$ and neglecting the resulting integration constant (implying that the particle starts from the point zero in the x-direction and with $v_x(0) = 0$). The perturbed wave magnetic field is expressed through the electric field $B_1 = kE_{z1}/\omega$.

The displacement and velocities in the three directions are coupled, however, taken separately, their nature is as follows. The dynamics in the z-direction is primarily due to the perturbed electric field. In the y-direction, the main dynamics is due to the $\boldsymbol{E}_1\times\boldsymbol{B}_1$-drift. On the other hand, this $\boldsymbol{v}_{y1}$ velocity is responsible for the $\boldsymbol{v}_{y1}\times\boldsymbol{B}_0$-Lorentz force in the x-direction.

Observe that in the limit of a small phase of $|\varphi| \equiv |ky - \omega t| \ll 1$, Eq. (5) can be rewritten in the form

$$\frac{\mathrm{d}^2 y}{\mathrm{d}\tau^2} + [\alpha_1 - 2\alpha_2(\tau)\cos(2\tau)]\, y = -2\alpha_2(\tau)\sin(2\tau). \tag{7}$$

Here, $y \equiv ky$, $z \equiv kz$, $\tau = \omega t/2$, and

$$\alpha_1 = 4\Omega^2/\omega^2, \quad \alpha_2(\tau) = \frac{ek\widehat{E}_{z1}}{m\omega^2}\frac{\mathrm{d}z}{\mathrm{d}\tau}.$$

Eq. (7) is the driven Mathieu equation which can have unstable solutions predicted by the Floquet's theorem.

One can also calculate how the distance between the two particles evolves in time due to the electromagnetic wave field. Using Eq. (4) for the two particles that are initially at positions $\boldsymbol{r}_1, \boldsymbol{r}_2$, respectively, after a few steps one obtains the following expression for the distance between the two particles in the y-direction (Vranjes 2011)

$$\frac{\mathrm{d}^2\delta y}{\mathrm{d}t^2} + \Omega^2\left[1 - \frac{v_{2,z}}{\Omega}\frac{\partial B_1(\boldsymbol{r}_1,t)/B_0}{\partial y}\right]\delta y = \Omega\frac{\mathrm{d}\delta z}{\mathrm{d}t}\frac{B_1(\boldsymbol{r}_1,t)}{B_0}. \tag{8}$$

Hence, the perpendicular distance δy between the two particles is determined by the parallel velocity of one of the particles. The distance can grow in time and this is equivalent to stochastic heating (Bellan 2006). This happens provided that

$$\delta \equiv \frac{v_{2,z}}{\Omega B_0}\frac{\partial B_1(\boldsymbol{r}_1,t)}{\partial y} > 1. \tag{9}$$

Evidently, some critical value for the parallel velocity $v_{2,z}$ is required. In the first approximation $v_{2,z} = eE_{z1}/(m\omega_r)$, and the condition (9) can be rewritten as

$$\delta \simeq \frac{k^2\widehat{E}_{z1}^2}{\omega_r^2 B_0^2} > 1. \tag{10}$$

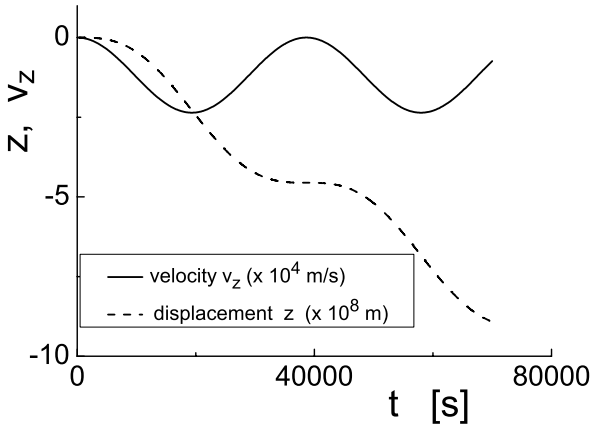

Fig. 1. Full line: proton velocity along the magnetic field vector, in the field of the wave $\widehat{E}_{z1}\sin(-\omega t + ky)$ for $\widehat{E}_{z1} = 2\times10^{-8}$ V/m, $\omega_r = 0.0001625$ Hz. Dashed line: the corresponding proton displacement along the magnetic field vector.

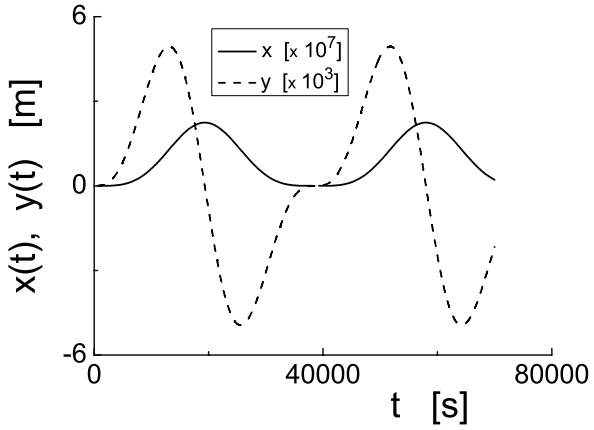

Fig. 2. The displacement in the x, y-plane, corresponding to the dynamics in Fig. 1, for $\widehat{E}_{z1} = 2\times10^{-8}$ V/m.

It will be shown that these conditions are in fact very easily satisfied, and, as a result, the particle motion in the wave field becomes stochastic for very small amplitude of the wave.

To describe more closely how the wave affects the particle, its dynamics will be presented for two different wave amplitudes. The equations are solved for the above given set of plasma parameters and first assuming a very small wave electric field amplitude of $\widehat{E}_{z1} = 2\times10^{-8}$ V/m only, and for the following arbitrary initial conditions: $x_0 = y_0 = z_0 = 0$, $v_{z0} = v_{x0} = 0$, $v_{y0} = 1$ m/s. The maximum time is set to some arbitrary value $t_m = 7\times10^4$ s. The particle velocity along the magnetic field vector v_{z1}, presented in Fig. 1, is a simple harmonic curve. However, the corresponding displacement of the particle along the magnetic field within one wave-period is huge, around half million kilometers. The particle is in fact subject to continuous directed drift along the magnetic field vector although the wave parallel electric field is oscillatory.

Due to the nonlinear Lorentz force, the motion in the perpendicular direction is affected and this is presented in Fig. 2 for the same value of the wave electric field $\widehat{E}_{z1} = 2\times10^{-8}$ V/m.

For one order of magnitude stronger wave electric field $\widehat{E}_{z1} = 2\times10^{-7}$ V/m, the particle displacement and velocity after some time become stochastic. With the assumed set of parameters this happens after about $t_s = 8.9$ h, i.e., within the time

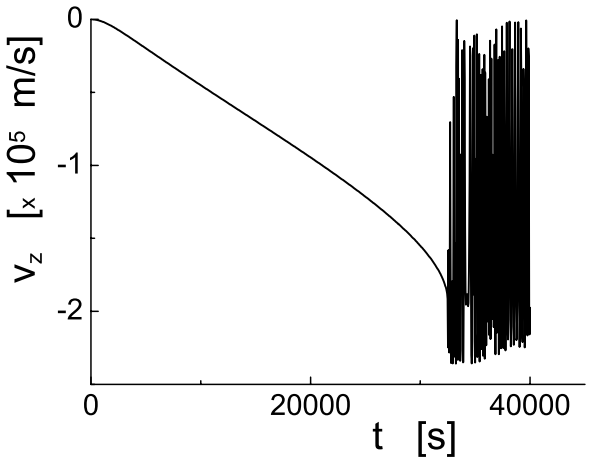

Fig. 3. Proton velocity along the magnetic field vector in the wave field with the amplitude of the electric field $\widehat{E}_{z1} = 2 \times 10^{-7}$ V/m. Stochastic motion develops after 8.9 h.

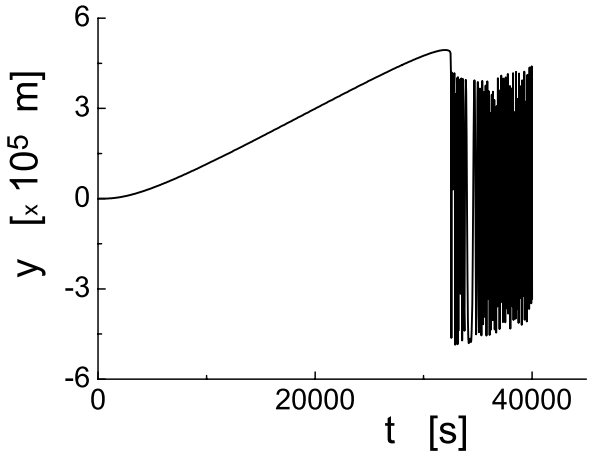

Fig. 4. Proton drift in the perpendicular y-direction (in the ecliptic plane or parallel to it) corresponding to Fig. 3, with the stochastic motion.

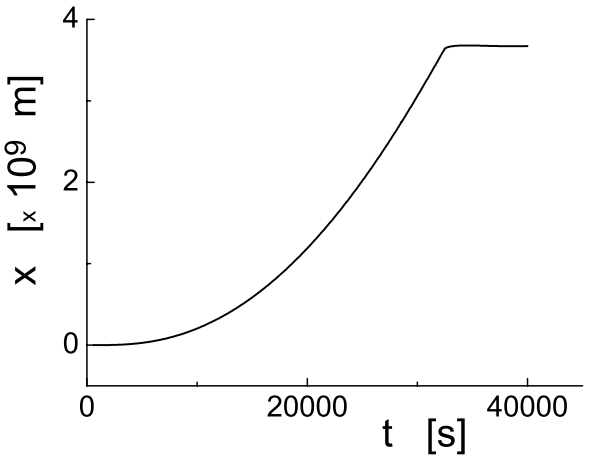

Fig. 5. Drift in the perpendicular x-direction, along the background density gradient, corresponding to Figs. 3, 4.

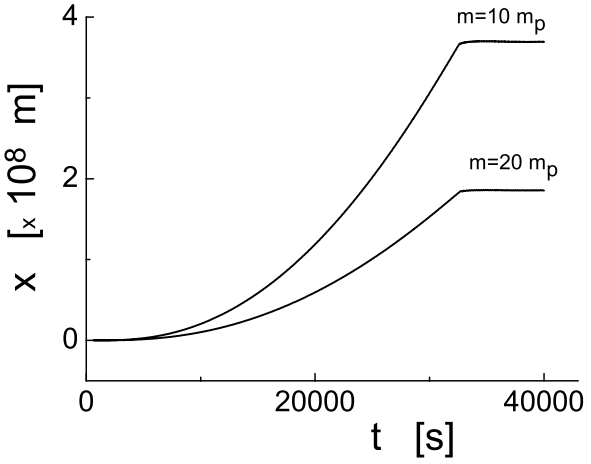

Fig. 6. Drift in the wave field in the direction of the density gradient (perpendicular to the magnetic field) for two ion species.

shorter than one single wave-period. Note that this value of $\widehat{E}_{z1}$ is still within the conventional assumption of small (linear) perturbations, which in the present case yields $e\phi/(\kappa T_e) = 2.5 \times 10^{-3}$, where ϕ is the wave potential corresponding to the given electric field and the wave number k. In the same time, for the assumed parameters, the condition (9) yields $\delta = 2.4$, so that the particle motion is in agrement with the theory (Vranjes 2011). Details on the particle dynamics in this regime are presented in Figs. 3–6. In accordance with Eq. (9), the particle moving along the magnetic field vector after some time is accelerated to large enough velocity v_z and its motion becomes stochastic, see Fig. 3. In the same time the mean velocity in the y-direction is stochastic and symmetric around zero, similar to the y-displacement presented in Fig. 4.

A particularly interesting feature is the displacement along the density gradient (in the direction perpendicular to the ecliptic plane or in any other one satisfying the assumed geometry) which is presented in Fig. 5. It turns out to be of the same order as the corresponding displacement in the z-direction (i.e., along the wave electric field vector and the magnetic field vector). Observe that the x-displacement remains constant after the development of the stochastic motion in the other two directions. However, the particle has already moved a few million kilometers along the density gradient (e.g., towards larger latitudes from the ecliptic plane). For the given distance and time from the graph, the average drift (diffusion) velocity is around $v_D = 1.2 \times 10^5$ m/s, implying an effective diffusion coefficient $D_\perp = v_D L_n = 1.2 \times 10^{13}$ m^2/s. Note that this estimate is for the least favorable case, i.e., for the particles with zero starting velocity in the z-direction. For larger values of $v_z(0)$ the effective diffusion can be increased, as will be shown later in the text.

It can be shown that for a larger electric field amplitude the stochastic behavior can be delayed, and this is clearly due to the following. The parallel velocity is obtained from the equation equivalent to (6)

$$\frac{\mathrm{d}v_z}{\mathrm{d}t} = \left(1 - v_y k/\omega\right) qE_{z1}/m, \tag{11}$$

while the condition (10) is obtained by using the linearized relation between the parallel velocity and the electric field (i.e., the first term in Eq. (11) only). However for a larger electric field and for a larger v_y, the nonlinear corrections should be kept. Indeed, for the previously used $E_{z1} = 2 \times 10^{-7}$ V/m, at $t = 3 \times 10^4$ s we have $v_z \simeq 155 \times 10^3$ m/s and $v_y \simeq 14$ m/s. On the other hand for a slightly larger $E_{z1} = 3 \times 10^{-7}$ V/m, at the same moment $t = 3 \times 10^4$ s, these velocities are $v_z \simeq 112 \times 10^3$ m/s and $v_y \simeq 23$ m/s. Therefore more time is required for the onset of stochastic behavior (i.e., for the particle to achieve the critical

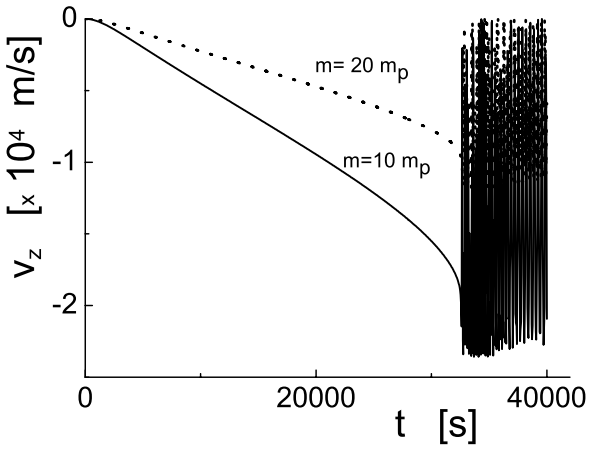

Fig. 7. Displacement in the direction of the magnetic field for the two ion species from Fig. 6.

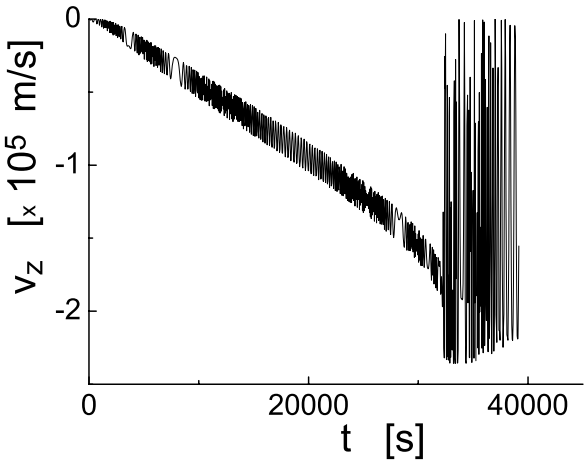

Fig. 8. The velocity along the magnetic field vector for $v_y[0] = 10^4$ m/s.

velocity v_z, see Eq. (9)), and it turns out that in the latter case this is around $t \simeq 54\,000$ s, i.e., after 15 h. In the same time the particle drift in the x-direction can become considerably larger and till this same moment $t = 3 \times 10^4$ s, the particle has already drifted in the direction of the density gradient for 1.4×10^{10} m. These are rough estimates and may be far from reality because nonlocal effects in the x-direction, and the finite extent of the mode in the same direction, should be taken into account.

3.1. Higher frequencies, larger electric field amplitudes

The wave frequency is increased by a factor 10, i.e., the wave period becomes 1.07 h, by reducing L_n by the same factor.

Increasing the electric field amplitude by the same factor, i.e., to $E_{z1} = 2 \times 10^{-6}$ V/m, the particle dynamics remains similar, yet, compared to Figs. 3, 4, the stochastic behavior develops after the time period reduced by the same factor, i.e., after 0.89 h. In the same time the displacement in the x-direction becomes shorter for one order of magnitude, as compared to Fig. 5.

3.2. Particle mass effects

Assuming heavier ions with the mass $m = \mu m_p$, and keeping all other parameters as before, the frequency (2) obviously remains nearly the same. However, the velocity along the magnetic field vector is reduced by $\sim 1/\mu$, as expected from Eq. (6). In the same the displacement in the x-direction is reduced by the same factor, as compared to Fig. 5. These effects are presented in Figs. 6, 7. Hence, the heavy ions arrival to some point in the space should be delayed as compared to protons, as frequently observed (Huttunen-Heikinmaa et al. 2005).

The same analysis may be performed for electrons too. Roughly speaking the result shows the effective diffusion coefficient $D_\perp$ which is for the mass ratio m_i/m_e larger than the value given in the text above, making it practically equal to the values obtained by direct observations (Wibberenz & Cane 2006; Zhang et al. 2003a), i.e., around 10^{17} m^2/s, and this even for the starting velocity $v_z(0) = 0$.

3.3. Effects of the starting velocity of the particle

The visually smooth parts of the curves in the previous figures in fact contain small fluctuations due to the particle gyro-motion, which for larger starting velocities of the particle become visible.

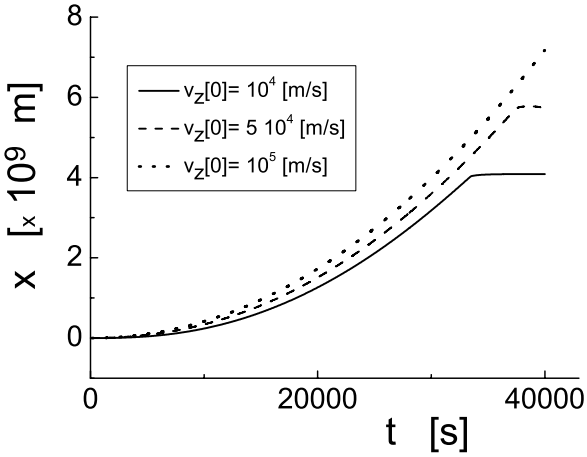

Fig. 9. Drift perpendicular to the magnetic field, for three different starting velocities $v_z(0)$ in the direction of the background magnetic field.

This is demonstrated in Fig. 8, where the velocity $v_y(0) = 10^4$ m/s, thus increased for four orders of magnitude as compared to the previous figures. However, as it is seen, the general picture is not changed. It turns out also that the displacement of the particle in the z and x directions remains practically unchanged, and this remains so for even larger starting velocity $v_y(0)$.

The situation is different when the starting velocity $v_z(0)$ is changed. This is demonstrated in Fig. 9, where the displacement in the direction of the density gradient is presented for three values $v_z(0) = 10^4$, 5×10^4, 10^5 m/s (full, dashed and dotted lines, respectively), and all other parameters are the same as before. Compare this also with the case $v_z[0] = 0$ from Fig. 5. A similar test is done by taking $v_z(0) = 10^6$ m/s; within 19 h the particle drifts to $x \simeq 3 \times 10^{10}$ m, i.e., to 0.2 AU.

Hence, it may be concluded that the particles that are initially faster will precede the rest of the plasma particles in their drift (diffusion) across the magnetic field.

4. Summary

The transverse drift wave is studied and its possible role in the transport of plasma particles. The mode is driven by the density gradient that should be ubiquitous in the solar wind (Bavassano et al. 1978; Tsiklauri et al. 2002) to which the model is applied.

Observations by the Ulysses spacecraft indicate an easy particles transport across the mean heliospheric magnetic fields, i.e., in the directions of the density gradient, that can not be explained by standard theory. In addition, simultaneous measurements in the ecliptic plane (by the Advanced Composition Explorer (ACE)) and at high latitude (Ulysses) in fact show the presence of SEP events at both spacecraft (Lario et al. 2003). With respect to this, the analysis performed in the work shows that very small values of the perturbed electric field of the transverse drift wave are required to have enormously large particle drift across the magnetic field. The drift depends on both the starting velocity of the particle, and its mass, yet it acts on all particles so that one may speak about the plasma transport in the direction perpendicular to the magnetic field. In the wave field the primary plasma motion is along the electric field vector, i.e., along the magnetic field vector. However, this component is coupled to the perpendicular drift motion, which appears to be of the same order (for the critical value of the wave electric field amplitude).

From Figs. 6 and 9 it follows that the transport will not be equally efficient for all particles. In a fraction of the wave period, in the first instance it will act on a small part of the plasma population from a unit volume, and those particles will effectively be transported by the wave. On the other hand, the wave occupies some space in both the perpendicular and parallel directions, and a cumulative effect of all of these particles that react first will result in the measured fluxes. However, at larger time scales this will have a negative feedback onto the wave, whose amplitude will reduce in time and the effect will necessarily cease. Some similar features are known from numerical simulations dealing with the oblique drift waves; the wave driven by the density gradient necessarily leads to the flattening of the density profile, and in time the wave perturbation should vanish. This relaxation of the density distribution is a well known fact. Yet the relaxation time is practically always large enough to have all the usual effects caused by the drift wave (i.e., heating, transport, stochastic phenomena) that are well documented and verified in laboratory experiments. The observed perpendicular fluxes are typically impulsive and with profiles that are sharp peaks followed by extended tails within which the fluxes in the end vanish. Simultaneous measurements by satellites at rather different latitudes (e.g., in the ecliptic plane and far from it) show very similar profiles. These extended tails in the flux profiles may in fact be the consequence of what is described above. Note also that according to Fig. 5 and the related paragraph in the manuscript, the transport in both x and z directions may be of the same order, and this could explain the mentioned similarities in the flux tail profiles in the ecliptic plane and in the direction perpendicular to it.

An additional property of the particle motion is that when the parallel velocity becomes large enough, all three velocity components change drastically, showing some stochastic features that will effectively increase the collisions in the environment and additionally contribute to the diffusion. The demonstrated drift and expected increased effective collision frequency, both caused by the wave instability, implies that standardly assumed frozen-in assumption may be far from reality.

The mechanism proposed here can act alone and/or in combination with some other phenomena like shocks that are also known to accelerate particles (Sandroos & Vainio 2009; Kuramitsu & Krasnoselskikh 2005; Aran et al. 2007). Together, the two phenomena may transport particles to high altitudes and provide physical explanation for the observations of solar energetic particles at high latitudes. The physics behind such events has been a challenge for the theory in the past. However, the solar wind is a very dynamic environment where an enormous amount of phenomena is continuously taking place, and this within a large span of the time and space scales. Among others, these include the instabilities caused by newborn ions originating from the pickup neutrals, that have been studied in the past 40 years. The growth time of such instabilities (Wu & Davidson 1972; Wu & Hartle 1974) can be a few hundred of seconds only, but they can also have wavelengths that are measured up to about 10^{10} m (Joyce et al. 2010). Some other phenomena imply heating in the solar wind (Smith et al. 2001; Gary et al. 2006; Breech et al. 2009), with the effects of the temperature anisotropy $T_\perp > T_\parallel$, and $T_\perp < T_\parallel$, where $\perp, \parallel$ stand for the perpendicular and parallel directions with respect to the ambient magnetic field vector, respectively, and with numerous evidences for $T_{\perp\alpha} > T_{\perp p}$, $T_{\parallel\alpha} > T_{\parallel p}$, where α, p denote respectively the alpha particles and protons (Tam & Chang 1999; Gary et al. 2006; Kasper et al. 2008). Nonlocal effects (i.e., the departure from the constant gradients used in the present model) can also affect the transport predicted in the model. Some of these and other phenomena, that can possibly affect the results presented here, can be dealt with analytically and this will be done in future studies, while some require numerical simulations.

References

Aran, A., Lario, D., Sanahuja, B., et al. 2007, A&A, 469, 1123
Bavassano, B., Dobrowolny, M., & Moreno, G. 1978, Solar Phys., 57, 445
Bellan, P. M. 2006, Fundamentals of Plasma Physics (Cambridge: Cambridge Univ. Press)
Breech, B., Matthaeus, W. H., Cranmer, S. R., Kasper, J. C., & Oughton, S. 2009, J. Geophys. Res., 114, A09103
Chen, F. F. 1988, Introduction to Plasma Physics and Controlled Fusion (New York: Plenum Press), 172
Dwyer, J. R., Mason, G. M., Mazur, J. E., et al. 1997, ApJ, 490, L115
Gary, S. P., Yin, L., & Winske, D. 2006, J. Geophys. Res., 111, A06105
Gosling, J. T. 2007, in Encyclopedia of the Solar System, ed. L. A. McFadden, P. R. Weissman, & T. V. Johnson (San Diego: Elsevier)
Huttunen-Heikinmaa, K., Valtonen, E., & Laitinen, T. 2005, A&A, 442, 673
Joyce, C. J., Smith, C. W., Isenberg, P. A., Murphy, N., & Schwadron, N. A. 2010, ApJ, 724, 1256
Kasper, J. C., Lazarus, A. J., & Gary, S. P. 2008, Phys. Rev. Lett., 101, 261103
Kóta, J., & Jokipii, J. R. 1995, Science, 268, 1024
Krall, N. A. 1972, in Advances in Plasma Physics, ed. A. Simon, & W. B. Thompson (New York: Interscience)
Krall, N. A., & Rosenbluth, M. N. 1963, Phys. Fluids, 6, 254
Krall, N. A., & Tidman, D. A. 1969, J. Geophys. Res., 74, 7439
Kuramitsu, Y., & Krasnoselskikh, V. 2005, A&A, 438, 391
Lario, D., Roelof, E. C., Decker, R. B., & Reisenfeld, D. B. 2003, Adv. Space Sci., 32, 579
Maclennan, C. G., Lanzerotti, L. J., & Gold, R. E. 2003, Geophys. Res. Lett., 30, 8033
Mikhailovskii, A. B. 1992, Electromagnetic Instabilities in an Inhomogeneous Plasma (London: IOP Pub.), 40
Sandroos, A., & Vainio, R. 2009, A&A, 507, L21
Smith, C. W., Matthaeus, W. H., Zank, G. P., et al. 2001, J. Geophys. Res., 106, 8253
Tam, S. W. Y., & Chang, T. 1999, Geophys. Res. Lett., 26, 3189
Tsiklauri, D., Nakariakov, V. M., & Arber, T. D. 2002, A&A, 395, 285
Vranjes, J. 2011, MNRAS, 415, 1543
Vranjes, J., & Poedts, S. 2006, A&A, 458, 635
Vranjes, J., & Poedts, S. 2009a, EPL, 16, 092902
Vranjes, J., & Poedts, S. 2009b, MNRAS, 398, 918
Wibberenz, G., & Cane, H. V. 2006, ApJ, 650, 1199
Wu, C. S., & Davidson, R. C. 1972, J. Geophys. Res., 77, 5399
Wu, C. S., & Hartle, R. E. 1974, J. Geophys. Res., 79, 283
Wu, C. S., Shi, B. R., & Zhou, G. C. 1986, Phys. Fluids, 29, 1840
Zhang, M., Jokipii, J. R., & McKibben, R. B. 2003a, ApJ, 595, 493
Zhang, M., McKibben, R. B., Lopate, C., et al. 2003b, J. Geophys. Res., 108, 1154